Food Hydrocolloids 174 (2026) 112348

Contents lists available at ScienceDirect

Food Hydrocolloids

journal homepage: www.elsevier.com/locate/foodhyd

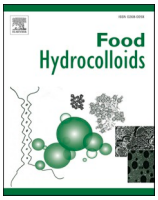

Emulsions stabilised with cellulose microfibrils and potato protein

Ieuan Roberts-Harry [a,b,*], Pau Marquès Duran [a,1], Max Molendijk [a], Daniel Bonn [b], Krassimir P. Velikov [a,b,c,**]

[a] Unilever Innovation Centre Wageningen, Bronland 14, Wageningen, 6708 WH, the Netherlands
[b] Institute of Physics, University of Amsterdam, Science Park 904, 1098 XH, Amsterdam, the Netherlands
[c] Soft Condensed Matter, Debye Institute for Nanomaterials Science, Utrecht University, Princetonplein 5, 3584 CC, Utrecht, the Netherlands

ARTICLE INFO

Keywords:
Emulsions
Cellulose microfibrils
Oscillatory rheology
Confocal laser scanning microscopy
Protein

ABSTRACT

We investigate oil-in-water emulsions prepared using potato protein and cellulose microfibrils (CMF) in the continuous phase. The ratio of potato protein and CMF is varied, along with the pH of the emulsion, and the volume fraction of the dispersed oil phase. We study how these factors affect the microstructure and flow properties of the emulsion, and link oscillatory rheology data to the microstructure via confocal laser scanning microscopy, cryo-scanning electron microscopy, and droplet size measurements. We find that the concentration of CMF is the key contributor to the flow properties of the continuous phase. While the protein has little effect on the rheology of the continuous phase, it plays a significant role in the flow properties of the emulsion. At low concentrations of protein, the CMF stabilises the emulsion droplets, and as the concentration of potato protein increases,this results in a decrease in droplet size, and an increase in emulsion elasticity. We find that it is also possible to drastically tune the elasticity of the emulsion via acidification. This is due to a combination of several different mechanisms, including altering the degree of attachment between droplets and the gel matrix. We finally investigate the dependence of elasticity on the oil fraction, and find that storage modulus increases for emulsions at pH 4, and decreases at neutral pH. Emulsions with adjustable elasticity offer a highly versatile system, enabling their use in the reformulation of various food emulsions.

1. Introduction

Emulsions are ubiquitous within the food industry; dairy cream, mayonnaise, and cream cheese are all examples of food emulsions. A large contributor to the sensory experience associated with such products is their texture and flow properties (Joyner, 2018). Volume fraction of the dispersed oil phase, droplet size, continuous phase rheology, and colloidal interactions within the emulsion are all known to contribute to emulsion rheology (Derkach, 2009; Pal, 2011). To form stable emulsions, particles or emulsifiers are typically used to adsorb at the oil-water interface and provide steric hindrance to coalescence. The most common emulsifiers used for oil-in-water type food products are proteins, with dairy- and egg-derived emulsifiers being employed most often. However, as plant-based diets become increasingly popular, plant-proteins, such as soy (Huang et al., 2024), faba (Liu et al., 2022), pea (Olsmats & Rennie, 2024), and potato (Bhutto et al., 2024) have been well studied as emulsifiers. While various plant proteins have been explored, their functionality can vary a lot based on their solubility. Potato protein isolate that is rich in patatin is particularly attractive as an emulsifier. It is highly soluble and has shown good emulsifying properties, as well as good foaming and gelling functionality (Tan et al., 2023). It is a globular protein, with an isoelectric point (IEP) of 4.9, and a molecular weight range of 45–50 kDa (Waglay & Karboune, 2016).

Water soluble polysaccharides typically show low surface activity and are commonly used as thickening agents in the continuous phase of emulsions to restrict droplets from creaming, and to enhance the sensory perception of the product. Cellulose microfibrils (CMF), a water insoluble polysaccharide, however, can be used both as a thickener and as Pickering stabiliser to emulsions (Miao et al., 2020; Yuan et al., 2021). CMF is a fibrillar form of cellulose, made of β-1,4-glucan chains

This article is part of a special issue entitled: 22nd Gums and Stabilisers published in Food Hydrocolloids.

* Corresponding author. Unilever Innovation Centre Wageningen, Bronland 14, Wageningen, 6708 WH, the Netherlands.
** Corresponding author. Unilever Innovation Centre Wageningen, Bronland 14, Wageningen, 6708 WH, the Netherlands.
E-mail addresses: ieuan.robertsharry@unilever.com (I. Roberts-Harry), Krassimir.velikov@unilever.com (K.P. Velikov).
[1] Current address: Intersnack Netherlands B.V. Havenstraat 62, 7005 AG Doetinchem, Netherlands.

https://doi.org/10.1016/j.foodhyd.2025.112348
Received 8 August 2025; Received in revised form 6 November 2025; Accepted 9 December 2025
Available online 10 December 2025

(Chinga-Carrasco, 2011). Hydrogen bonding between these chains results in highly crystalline structure. The microfibrils are very attractive toward one another, driven by hydrogen bonding and van der Waals interactions (Moon et al., 2011). CMF are present in all fruit and vegetable tissues, purees and in insoluble dietary fibres (e.g. in citrus fibre), and can be produced by bacteria and some algae. In citrus fibre, CMF is present along with hemicellulose, proteinaceous material and pectin (Fechner et al., 2013). The CMF derived from insoluble dietary fibre are not chemically modified. Previous studies have also demonstrated how the CMF obtained from citrus fibre (CF) can be used alone to stabilise emulsions (Nomena et al., 2018, 2021; Wallecan et al., 2015). In addition to its structuring and stabilising properties, CMF are an advantageous material from a sustainability point of view, as they can be recovered from the waste or side streams of fruit processing procedures (Costa et al., 2018; Naz et al., 2016; Wallecan et al., 2015). From a nutrition perspective, CMF are a non-digestible, non-fermentable material (Mudgil & Barak, 2013), and so can be useful in the development of low calorie foods.

Despite the well-established dual role of CMF as a bulk and interfacial stabiliser, the research on cellulose fibrils in combination with plant proteins has been limited to the use of bacterial cellulose and soy protein (Wang et al., 2025; Zhang et al., 2022; Zhu et al., 2025). The use of plant-derived CMF and plant protein has not been studied. In this paper, we study the use of potato protein as emulsifier, and CMF present in CF dispersions as both emulsifier and bulk structurant to stabilise oil-in-water (O/W) emulsions. The aim of the study is to understand the link between the microstructure of the system and its flow properties, which can allow for the design of a wide range of plant-based alternatives with different textures. By using both materials together, we prepare emulsions which have tuneable flow properties, specifically elastic modulus, which is less easily achieved using either of the materials alone to stabilise emulsions. We do this by altering the ratio of CMF and potato protein, pH, and volume fraction of oil, and elucidating the data with confocal laser scanning microscopy and cryo-SEM. We find that the emulsion flow properties can be tuned in several different ways, and that the CMF and the potato protein can act synergistically to stabilise the emulsion, though this is pH dependent. To the best of our knowledge, we are the first to discuss such an effect for emulsion prepared with cellulose microfibrils and protein. This versatility of this system could allow the formulation of plant-based alternatives of a variety of traditionally animal-based food emulsions.

2. Materials and methods

2.1. Materials

Citrus fibre Herbacel AQ + type N (65 wt% of cellulose, 3.7 wt% of hemicellulose, and 5 wt% of proteinaceous materials (Fechner et al., 2013)) from Herbafood Ingredients GmbH, Germany was used as a source of cellulose microfibrils. Potato protein isolate (PPI) Solanic 200 (according to supplier specification: 90 wt% protein, 0.2 wt% dietary fibre, 0.1 wt% lipids, 0.2 wt% carbohydrates) was obtained from Avebe. Soybean oil (Wijnimport van der Steen B.V.) was used. Sodium Hydroxide pellets were received from J.T. Baker and used to prepare a 5 wt % NaOH solution, and vinegar spirit (12 %) was purchased from Carl Keuhne KG GmbH CO. Antimicrobial agent Proxel GXL was kindly provided by Arxada. Calcoflour White and Nile Red, obtained from Sigma Aldrich were used as fluorescent dyes for the Confocal Laser Scanning Microscopy.

2.2. Methods

The aqueous continuous phase was prepared by dispersing citrus fibre (CF) powder in deionized water using a magnetic stirrer (Labotech EM 3300 T, Netherlands) for 5 min at a speed of 500 rpm. The initial pH of the dispersion, which was approximately 3.5–4.0 depending on the concentration of citrus fibre, was adjusted to 7.0. Varying concentrations (up to 1.0 wt%) of potato protein powder were added to the samples, while dispersing using a magnetic stirrer at 500 rpm for 5 min. To maximise protein dispersion and dissolution, a high-shear laboratory mixer (Silverson L5M, USA) was used at 2000 rpm, using a screen with 1 mm holes, for 1 min. The mixing was performed with the mixer head fully immersed in the sample to avoid incorporating air into the samples. The dispersion was then passed through a homogenizer (M110-S Microfluidizer, Microfluidics, USA) with a 200 μm diameter, Z-shape, ceramic channel operating at a pressure of 1000 bar. Following this stage, approximately 85 μg of Proxel GXL (Arxada, Switzerland) antimicrobial agent per gram of sample was added. Finally, the pH was adjusted by gently hand-stirring the vinegar spirit into the sample, such that shear had minimal effect on the microstructure. The pH was adjusted to 4, unless otherwise stated in the text.

For the preparation of the emulsions, soybean oil was added to the aqueous mixture of CF and potato protein prior to the homogenization with the Microfluidizer, as described in the preparation of the continuous phase. The oil was gradually added while dispersing with a Silverson L5M at 7000 rpm. Once the entirety of the oil was added, the emulsion was further dispersed for 5 minutes. Next, the emulsion was passed through the Microfluidizer, with the same parameters as detailed above. Antimicrobial agent was added, 85 mg per g of sample. Finally, the pH of the emulsion was adjusted as described above.

2.3. Rheology

Rheological measurements were carried out on each sample using a stress-controlled rheometer (MCR 302, Anton Paar, Austria). A sand-blasted, plate-plate geometry with a 50 mm diameter was used, with a 1 mm gap. Oscillatory rheology measurements were performed. An amplitude sweep was performed on the samples, increasing the amplitude logarithmically from 0.01 to 300 % strain, at a frequency of 1 radian/s. Next, frequency sweeps were completed, increasing the frequency from 1 to 100 rad/s, at an amplitude of 0.1 %, as it was found to be within the linear viscoelastic regime (LVER) of the samples during the amplitude sweeps.

2.4. Droplet size via time-domain NMR

Droplet sizes were measured using a Bruker mq20 minispec Nuclear Magnetic Resonance (NMR), using a protocol described previously (Goudappel et al., 2001). Using pulsed-field gradients, the constrained diffusion coefficient of triglyceride molecules inside the oil droplets is measured. Finally, this is modelled to a lognormal droplet size distribution assuming a spherical droplet size, through which we obtain the volume-weighted geometric-mean droplet diameter (d33). Cross-validation of the data generated was done using confocal laser scanning microscopy along with ImageJ's particle analyzer function, as well as cryo-SEM images. Discussion of this cross-validation is available in the supplementary material (Fig. S1).

2.5. Confocal scanning laser microscopy

Confocal scanning laser microscopy (CSLM) was performed on a Zeiss LSM 880 (Germany) confocal microscope, using a 63 × magnification with oil objective. The samples were stained by adding Nile Red (100 μL/g of sample) for the oil and Calcofluor White (64 μL/g of sample) for cellulose. The laser used to excite the Nile Red was 405 nm, and the laser used for the Calcofluor White was 514 nm. A sequential imaging protocol was used to prevent channel crosstalk. For imaging, the samples were placed between two cover slips. Image processing and analysis was performed with ImageJ.

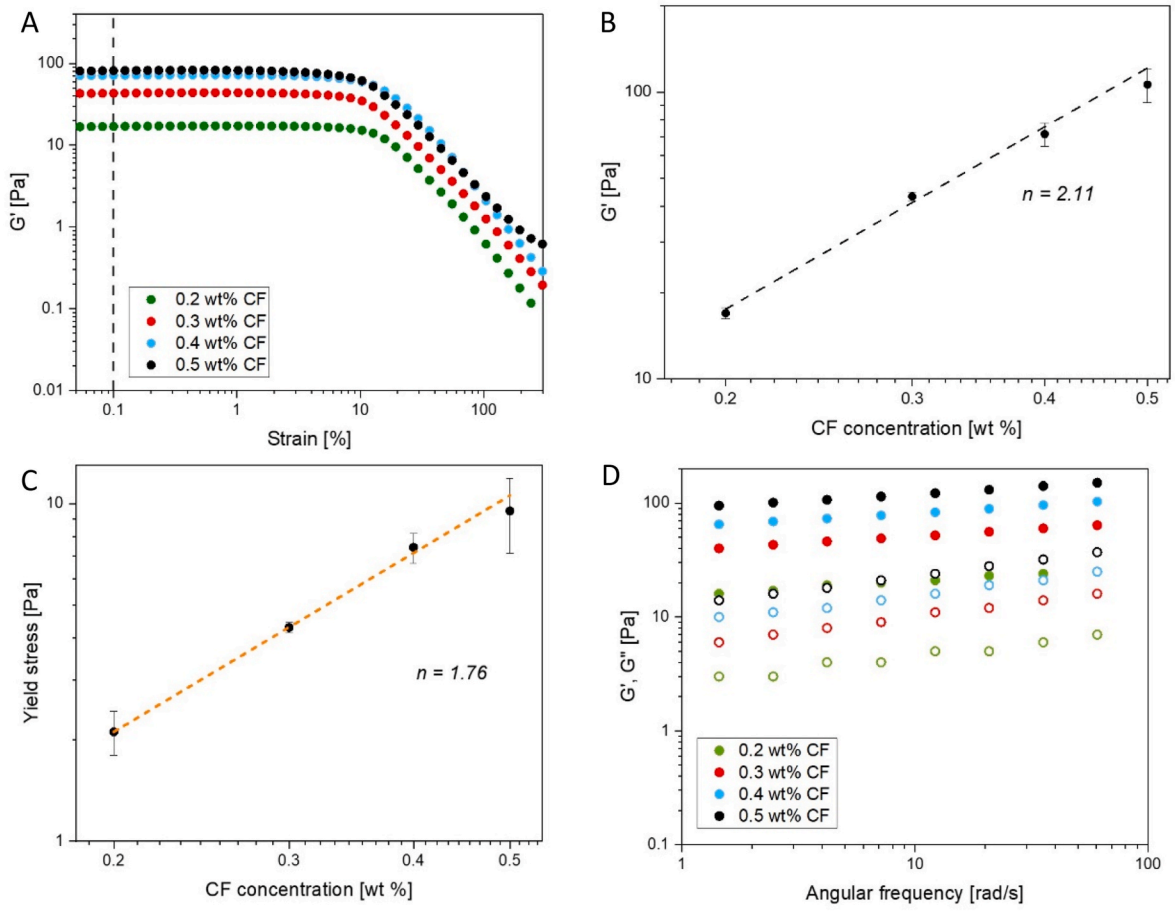

Fig. 1. A) Amplitude sweeps for gels prepared with increasing concentrations of citrus fibre (CF). Dotted line indicates the storage modulus (G′) at 0.1 % strain, demonstrating that it is within the linear viscoelastic regime (LVER). B) Storage modulus within the LVER, at 1 % strain, versus concentration of CF. Dotted line is G' ~ (wt% CF)$^{2.11}$. C) Yield stress plotted versus CF concentration, where yield stress (σ_y) is defined as the stress at which storage modulus (G′) equals the loss modulus (G″). Orange dotted line is $\sigma_y \sim$ (wt% CF) $^{1.76}$. D) Storage and loss modulus of emulsions with increasing concentration of fibre versus angular frequency (●- storage modulus, ○ – loss modulus). (For interpretation of the references to colour in this figure legend, the reader is referred to the Web version of this article.)

2.6. Cryo-scanning electron microscopy (Cryo-SEM)

Cryo-SEM was employed to further image the microstructure of the emulsions. A small droplet of sample was placed on a rivet and plunged into melting ethane, which flash freezes the entire sample. After freezing, the sample was placed into the prep-chamber of the SEM (Gatan Alto2500, USA), and the system was cooled with liquid nitrogen to a temperature of −125 °C. The frozen sample was cryo-fractured with a knife attachment in the prep-chamber. After fracture, the sample was heated to −90 °C for 90s to sublimate part of the ice to increase depth contrast. After sublimation, the sample was brought back to −125 °C. The sample was then sputter-coated with platinum for 90 s from a perpendicular angle, and another 30 s while tilting to ensure a uniform coating. The sample was then placed into the scanning electron microscope (Zeiss Auriga, Germany). The sample was viewed at 3 kV at 5 mm working distance with an SE2 detector under high vacuum at −125 °C.

3. Results and discussion

3.1. Continuous phase

The continuous phase of the emulsion was studied, and how both the citrus fibre (CF) dispersion containing cellulose microfibrils (CMFs) and potato protein contribute to the flow behaviour of the system. Samples with increasing concentration of CF (0.2–0.5 wt%, increments of 0.1 wt %) and no protein were prepared. The pH of all samples was adjusted to 4 using vinegar spirit. Amplitude sweeps for samples with increasing CF concentration are displayed (Fig. 1A), and the storage moduli at 0.1 % strain (i.e. within the LVER), are plotted versus concentration of the CF (Fig. 1B). All samples were found to be strain-weakening, even at the lowest concentration. The strain-weakening stems from the separation of CMF flocs, and alignment of fibrils in the direction of shear (de Kort et al., 2016; Karppinen et al., 2012). We observe a power-law relationship between the concentration of CF and the storage modulus, *G'*, as observed previously (Roberts-Harry et al., 2026). We find an exponent of $n = 2.11$ (Fig. 1B). This value is in line with other studies on dispersion of CMF from CF (Nomena et al., 2021). This demonstrates that the dependence of the storage modulus on concentration sits in an expected range, as models and theories for fibrous gels and semiflexible biopolymers predict an exponent of 2–2.5 (de Gennes, 1979; MacKintosh & Janmey, 1995).

The yield stress of the gels with increasing concentration of the CF is also displayed (Fig. 1C), where the yield stress is considered to be the value of stress when $G' = G''$ during the amplitude sweep, as discussed previously in the literature (Dinkgreve et al., 2016). The yield stress increases with concentration of the CF, with a power law exponent of 1.76. This is slightly lower than expected, as other authors have reported a scaling exponent of approximately 2, for CMF dispersions from CF, though processing conditions differed (Blok et al., 2021). Frequency sweeps demonstrated that the CF dispersions behave elastically at all concentrations ($G' > G''$), indicating that they are rheological gels. Furthermore, the samples are found to be almost independent of the

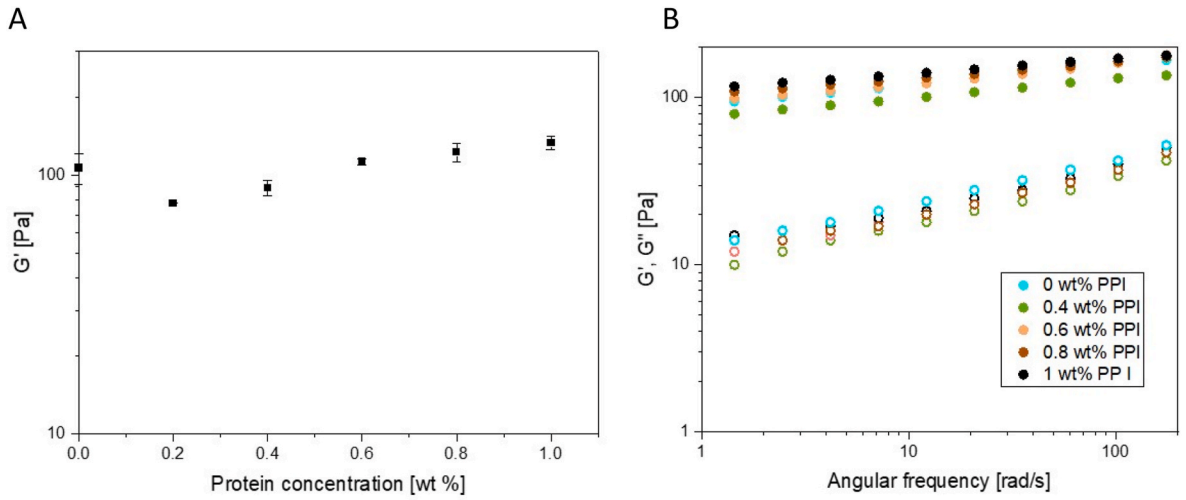

Fig. 2. A) Storage modulus within the linear viscoelastic regime, at 1 % strain, and B) frequency sweeps (●- storage modulus, ○ – loss modulus) for gels with 0.5 wt% citrus fibre dispersion and increasing amounts of potato protein isolate (PPI).

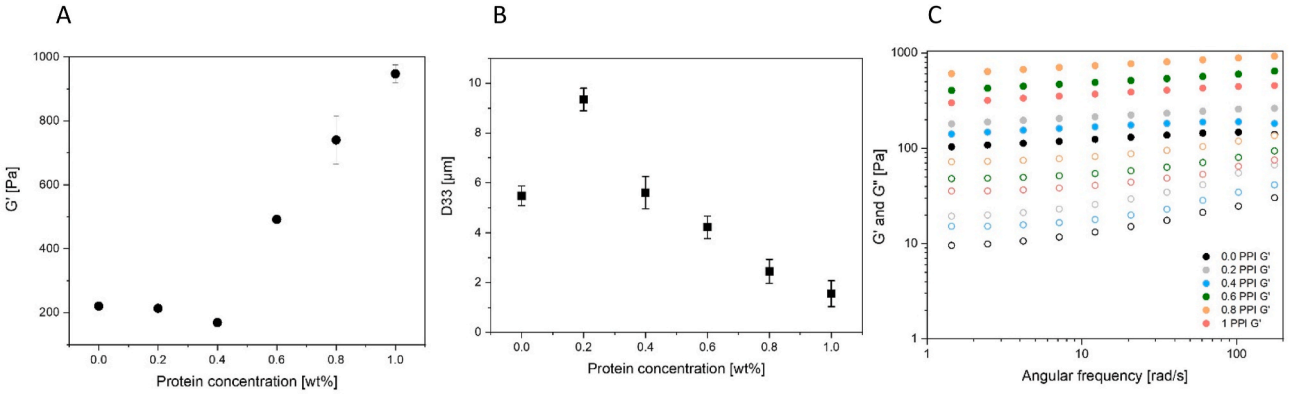

Fig. 3. A) Storage modulus (G′), B) droplet size and C) frequency dependence for emulsions prepared with 0.5 wt% citrus fiber and increasing concentration of potato protein isolate (PPI) in the continuous phase, and 30 wt% soybean oil.

frequency.

To establish the effect of protein addition to the rheology of the continuous phase, samples with increasing concentrations of protein (0–1 wt%, increments of 0.2 wt%), with a fixed concentration of CF (0.5 wt%), were prepared at pH 4. We find that changes in protein concentration have a small influence on the storage modulus of the gel (Fig. 2). We observe an initial small decrease in G′, which is then followed by a small linear increase at higher concentrations of potato protein (Fig. 2A). The small dip is attributed to the attraction between the protein, positively charged at pH 4, ad the CMF and pectin which are both negatively charged. The frequency sweep (Fig. 2B) demonstrates that the samples remain as rheological gels ($G' > G''$), almost independent of the frequency, at all concentrations of protein studied.

4. Emulsions

4.1. Influence of protein on the continuous phase

When emulsions are prepared with these materials, the concentration of protein has a much more profound impact on the rheology of the system. The storage modulus of emulsions with a constant amount of CF (0.5 wt%) and increasing amounts of potato protein (0–1 wt%) in the continuous phase, was recorded (Fig. 3A). Emulsification took place at pH 7, where both potato protein and CMF (and the present pectin) have negative charge, and then acidification to pH 4 where the protein reverse surface charge. At low concentrations of protein (≤ 0.4 wt%), the storage modulus remains fairly constant. However, we observe a steady increase in the storage modulus of the emulsion as protein concentration increases above 0.4 wt%. We find that the emulsion droplet size initially increases as a small amount of protein is added, from 0 to 0.2 wt% protein, and then decreases at higher concentrations of protein. The initial increase in droplet size is attributed to competitive adsorption to the oil-water face between the CMF and the protein. When there is no protein added, the droplets are stabilised solely by the CMF which adsorb to the droplet surface. As the concentration of protein in the continuous phase increases to 0.2 wt%, the protein adsorbs faster than the CMF and hinders its effective adsorption at the droplet interface during emulsification. However, there is not enough protein to adsorb and reduce the interfacial tension, and stabilise the oil droplets, which leads to decreased droplet size. Notably, the increase in droplet size from 0 to 0.2 wt% protein does not cause an increase in the storage modulus. Suggesting that for larger droplet size, it is the CMF network in the continuous phase that contributes most to elasticity of the sample. At higher concentrations of protein, the droplet size decreases, reaching as small as 1.6 µm at 1 wt% potato protein. This is because there is more protein to adsorb to the oil-water interface, thus reducing the interfacial tension of the oil-water interface (van Koningsveld et al., 2006). This decrease in droplet size drives an increase in the storage modulus. Above the values studied here, droplet size would eventually reach a plateau, as the interfacial tension reaches a minimum, for a given value of shear

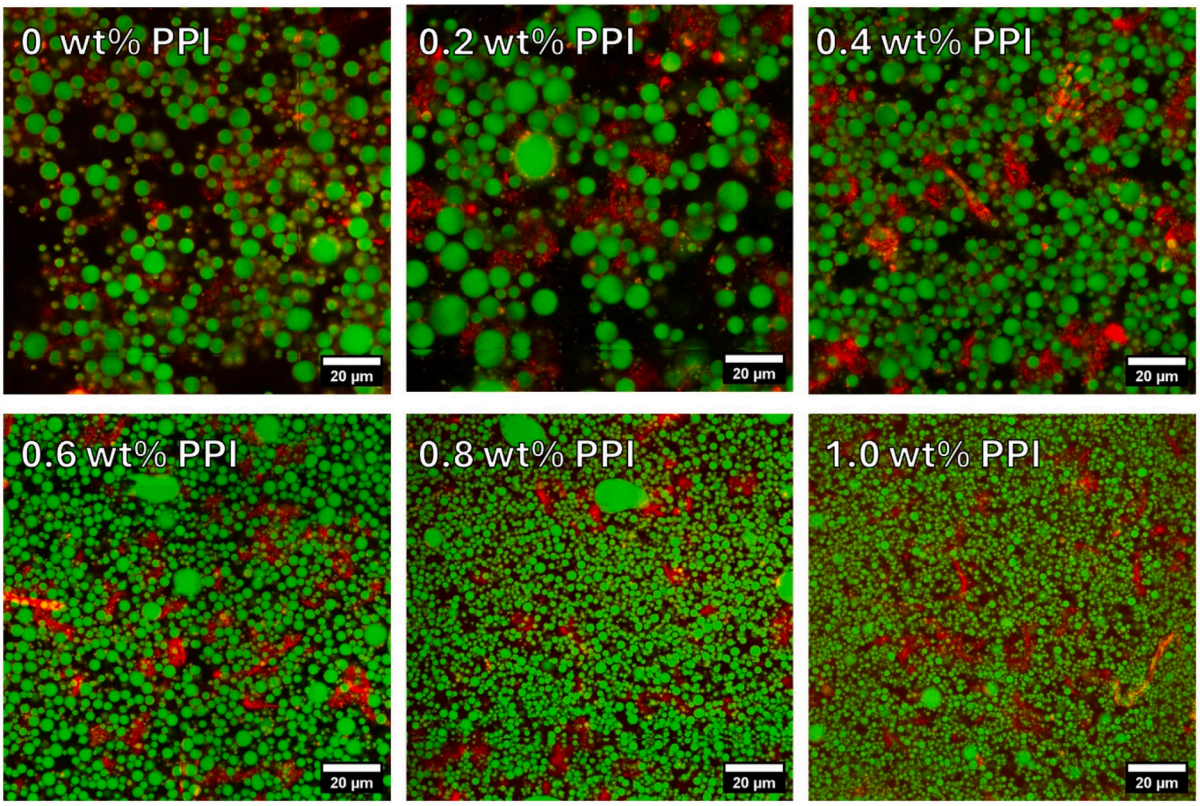

Fig. 4. Micrographs obtained via CSLM of emulsions with 0.5 wt% citrus fibre and increasing potato protein isolate (PPI) concentration, and 30 wt% soybean oil, at pH 4. The cellulose microfibrils are depicted in red, and the oil depicted in green. Readers are referred to the online version of the article for improved viewing of the images. (For interpretation of the references to colour in this figure legend, the reader is referred to the Web version of this article.)

applied for droplet break-up. This occurs as the amount of protein at the oil-water interface reaches a maximum, and no further protein can adsorb (Liu et al., 2024).

As mentioned previously, these measurements demonstrate that the storage modulus is independent of the droplet size at low concentrations of protein ($\leq$ 0.4 wt%). At this protein concentration, the droplets are larger, and therefore there are fewer droplets. Given that the emulsion is also quite dilute, droplet interactions do not contribute very much to sample rheology. Conversely, at higher values of protein, the droplet size and number of droplets are key drivers of increasing storage modulus. Droplet size is a known contributor to the rheology of concentrated emulsions, as it influences the interaction between droplets via their Laplace pressure, given by γ/r, where interfacial tension (γ) is divided by the droplet radius (r) (Princen & Kiss, 1986). In the supplementary information (S2), the elasticity of the emulsions is plotted against the droplet size, demonstrating how smaller droplet size drive an increase in emulsion elasticity. Similarly to the continuous phase, however, the frequency dependence of the emulsion was not affected by increasing protein concentration (Fig. 3C). At all concentrations, the emulsions were fairly insensitive to changes in frequency, and the

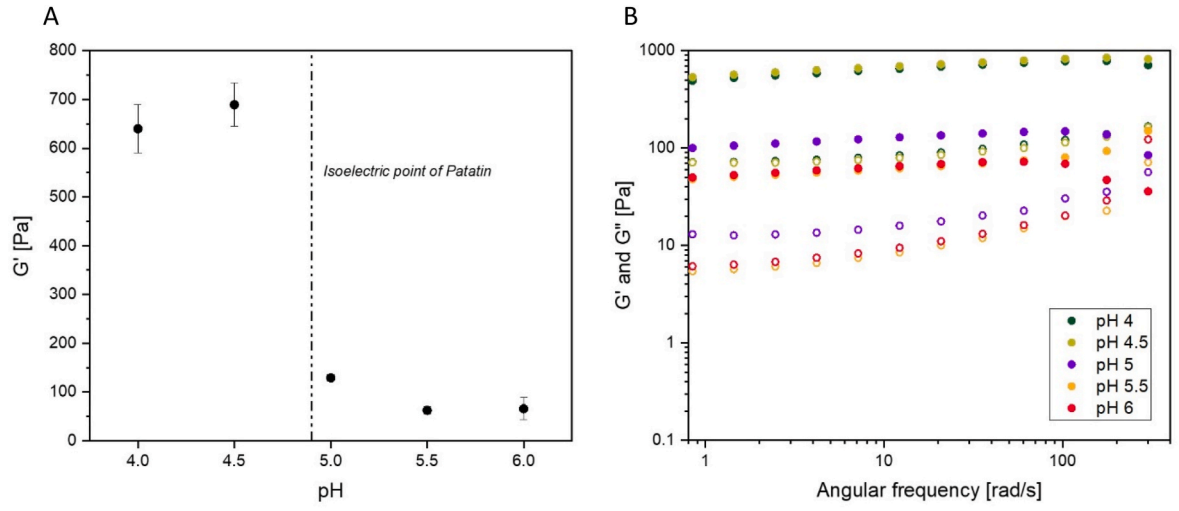

Fig. 5. A) Storage modulus in the linear viscoelastic regime and B) frequency dependence of storage and loss modulus for emulsions with 0.5 wt% CF and 1 wt% potato protein in the continuous phase, with varying pH.

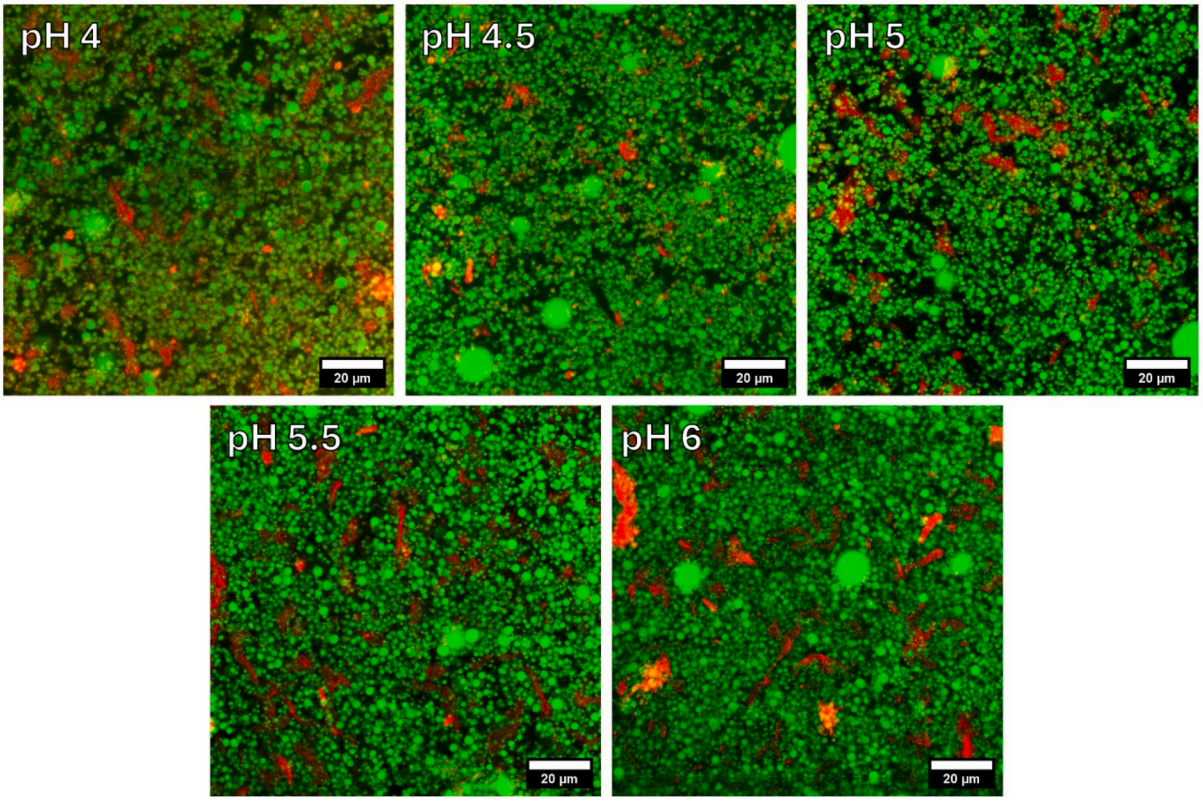

Fig. 6. Micrographs obtained via CSLM of emulsions with 0.5 wt% citrus fibre, 1 wt% potato protein, and 30 wt% soybean oil, at various pH. The cellulose microfibrils are depicted in red, and the oil depicted in green. Also shown is the measured dispersity index of emulsions at varying pH. Lines are to guide the eye. Readers are referred to the online version of the article for improved viewing of the images. (For interpretation of the references to colour in this figure legend, the reader is referred to the Web version of this article.)

storage modulus was higher than loss modulus for all concentrations, at all frequencies, indicating gel-like behaviour.

To further probe how the CMF and protein stabilise emulsions, confocal laser scanning microscopy (CSLM) was used to image the emulsion microstructure (Fig. 4). In the absence of potato protein, the CMF provide Pickering type of stabilisation to the emulsion, as some droplets are dispersed within flocs of the CMF, and droplets appear attached to flocs of the CMF, consistent with previous observations in the literature (Nomena et al., 2018). Droplets also appear flocculated, and this is caused by bridging flocculation via the CMF (Nomena et al., 2018; Yuan et al., 2021). In turn, this leads to a qualitatively observed heterogeneity in the dispersity of the emulsion droplets. As protein concentration increases above 0.4 wt%, and droplet size decreases, the droplets are more homogeneously dispersed.

4.2. pH dependence of emulsions

We then consider the effect that pH has on the properties of the emulsion. Emulsions with 0.5 wt% CF, 1 wt% potato protein in the continuous phase, and 30 wt% soybean oil were prepared. The final pH of the emulsion was altered using vinegar spirit, ranging between pH 4 and 6, as this pH range is most applicable for food emulsion applications.

We observe a significant influence of pH on the storage modulus of the emulsions (Fig. 5A). The storage modulus of the emulsion below pH 5 is high, ranging from 600 to 700 Pa, while at pH 5 and above, samples exhibited a drastically lower storage modulus, ranging from 50 to 125 Pa. Gels of CF with potato protein (i.e. without oil) were also prepared, the dependence of their elasticity on pH can be found in the supplementary information (S3). While storage modulus decreased from 200 Pa, it is not to the same extent as observed in the emulsions. With regard to the emulsion system, we observe no change in droplet size, remaining constant at approximately 1.75 μm (see Supplementary information, S4). This was anticipated as emulsification took place at pH 7, and the pH was adjusted after emulsification. Via frequency sweeps, we observe how the emulsions at higher pH are more fluid like, as they have a higher frequency dependence than at lower pH (Fig. 5B).

The observed increase in storage modulus with acidification is caused by three different mechanisms. The first is aggregation of the protein as the emulsion is being passed through its isoelectric point (IEP), which, for patatin, is 4.9 (Waglay & Karboune, 2016). At the isoelectric point, there is no net charge on the protein, and it is significantly less soluble (Krstonošić et al., 2020; Tan et al., 2023). As such, it aggregates, increasing the elasticity of the oil-water interface providing a more effective Pickering stabilisation to the droplets (Zhang et al., 2021). This renders the oil droplets more rigid, such that there is an increase of the storage modulus of the emulsion. The second contributing factor is that there is an increased attraction between the droplets, as there is no net charge on the protein at the droplet interface when at pH values close to the IEP of the protein. Emulsions prepared with just potato protein, without CMF, showed a drastic increase in the storage modulus at pH 5 (Supplementary information, S5). This demonstrates that pH induced changes in the protein structure and surface charge contribute significantly to the pH dependence of emulsion stability displayed in Fig. 5A. Thirdly, changes in pH alters the electrostatic interaction between the CMF, and the protein at the interface of the droplets. This leads to the droplets becoming interconnected with the CMF network (Figs. 8 and 10 wt% oil). As CMF have slight negative surface potential (Liu et al., 2024; Zhang et al., 2024), and the protein is at pH 6, i.e. above its IEP, is also negatively charged (Tan et al., 2023), there is a repulsion between the protein adsorbed at the oil-water interface and the CMF in the continuous phase. As the emulsion is acidified below the IEP of the potato protein, said protein becomes

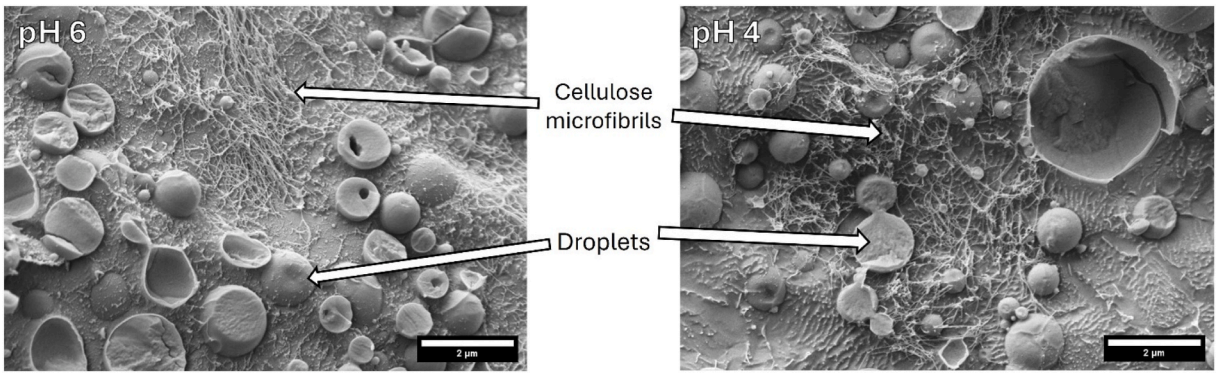

Fig. 7. Cryo-SEM images of samples of 0.5 wt % citrus fibre and 1 wt% potato protein isolate in the continuous phase, 30 wt% soybean oil, at pH 6 and pH 4. Scale bar is 2 µm.

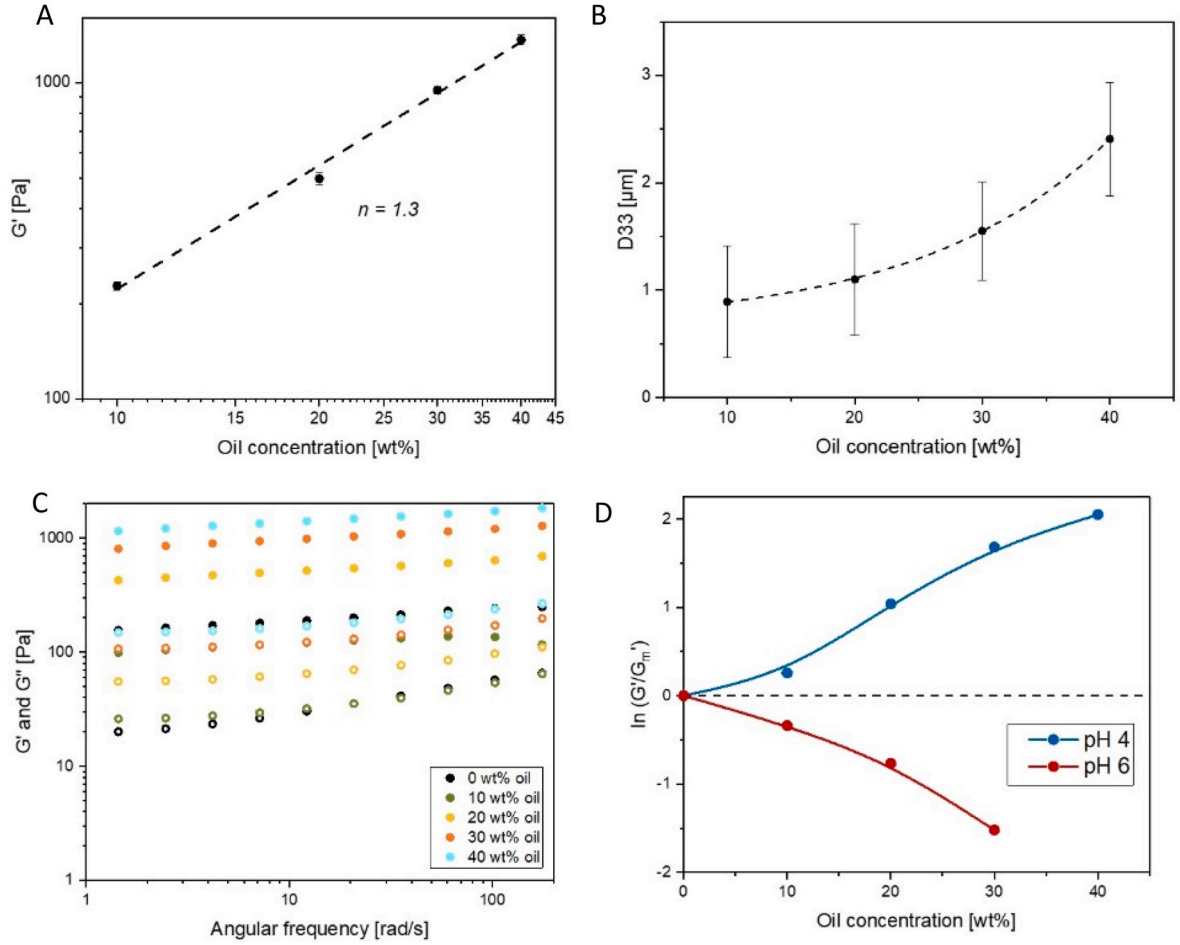

Fig. 8. A) Storage modulus within the LVER versus oil concentration for emulsion filled gels, where the dotted line represents power-law scaling with exponent n = 1.3. B) Droplet size plotted versus oil concentration, where dotted line represents exponential scaling. C) Frequency sweep for emulsions with 0.5 wt% CF and 1 wt% protein in the continuous phase and increasing concentration of soybean oil. Dotted lines are exponential fits. D) Logarithm of G'/G_m', where G_m' is the storage modulus of the continuous matrix (i.e. G′ at 0 % oil). Lines are to guide the eye.

positively charged, with values of approximately +20 mV being reported in the literature at pH 4 (Tan et al., 2023). This leads to an attraction between the oil droplets and the fibre network, such that the oil droplets and the fibre network are interconnected. As such, the droplets act as active fillers and contribute to an increase in the storage modulus, as previously discussed in the literature (Dickinson & Chen, 1999, Dickinson, 2012). From CSLM micrographs, the emulsion droplets appear more flocculated at pH 5, leaving large areas not occupied by droplets, as opposed to being homogeneously dispersed at other pH values (Fig. 6). We quantify the extent of flocculation of these droplets from the CSLM micrographs using an index of dispersity (IoD) (see Supporting information, Fig. S6), which other authors have discussed (Kam et al., 2013). The IoD value measures the spatial uniformity of the droplets (i.e. how uniformly droplets are dispersed across the micrograph), with higher values indicating a higher variation in droplet population, and hence degree of droplet flocculation. The extent of

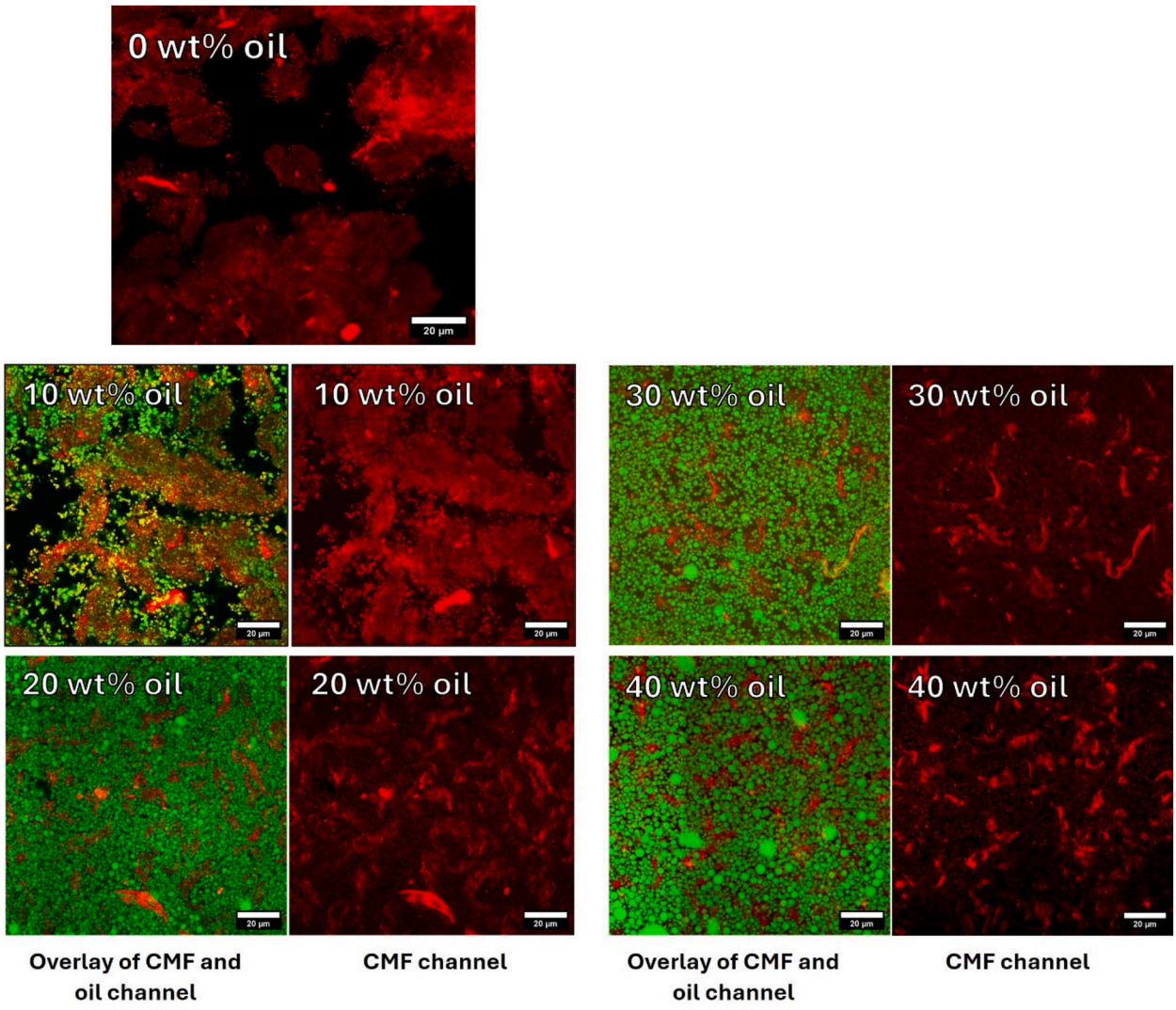

Fig. 9. Confocal laser scanning microscopy images of emulsions with 0.5 wt% citrus fibre and 1 wt% protein the aqueous phase, with increases amounts of oil dispersed (at pH 4). The overlay of the oil and fibre channels are shown, along with the fibre channel alone. The cellulose microfibrils are depicted in red, and the oil droplets in green. Scale bar is 20 μm. (For interpretation of the references to colour in this figure legend, the reader is referred to the Web version of this article.)

flocculation increases at pH 5, being very close to the IEP of the protein, such that the repulsive force between the droplets is diminished. Using cryo-SEM, we image samples above and below the IEP of the protein (Fig. 7). The images taken demonstrate that more CMF are drawn to the droplet interface when the emulsion is at pH 4, compared to pH 6.

4.3. Influence of oil volume fraction

Finally, we consider the effect increasing the volume fraction of the dispersed oil phase has on the flow properties of emulsions. Specifically, emulsions stabilised with 0.5 wt% CF, and 1 wt% potato protein, at pH 4. The storage modulus within the LVER increases with the oil concentration of the emulsion with a power law dependence, where the power law exponent $n = 1.3$ (Fig. 8A). As the oil fraction increases, droplet rearrangement becomes increasingly limited. They are able to contribute to the resistance to shear as the droplets and the gel matrix are attached, as discussed above. The droplet size, however, increases (Fig. 8B) with increasing oil fraction, which typically leads to a decrease in the storage modulus. This increase in droplet size is because the concentration of potato protein per unit droplet surface area decreases as oil concentration increases, but the total protein concentration in the sample remains the same. Furthermore, the increased viscosity due to increased oil fraction effectively can reduce the shear stress experienced per droplet, resulting in less effective droplet breakup.

We observe a small difference in the frequency dependence of G' with increasing oil fraction, as samples with a lower oil fraction show slight frequency dependence in comparison with samples at higher oil fraction. The ratio of the emulsion storage modulus to that of the continuous phase, with increasing oil fraction, for emulsions adjusted to pH 4 and 6 are plotted (Fig. 8D). While the ratio increases for the emulsion at pH 4, at pH 6 the opposite effect occurs. This is because at pH 6 the force applied to the system is not passed to the filler particle i.e. the oil droplets, as there is less attachment between the fillers and the gel matrix. These results also allow us to conclude that by varying pH, we alter how bound the oil droplets are to the gel matrix, as proposed previously.

Again, CSLM is used to study the emulsion microstructure at pH 4, and how the mechanism for emulsion stabilisation changes with increasing oil fraction (Fig. 9). An overlay of the channels used to image the CMF and the oil droplets is displayed, as well as the CMF channel alone. At low concentrations of oil, specifically at 10 wt% oil, there is a clear alignment of droplets to the CMF flocs present in the system, as there are no regions where the cellulose fibrils are present without droplets. CMF have been found to be surface active, but are also able to

provide steric stabilisation to emulsions by thickening the aqueous phase, and providing a yield stress (Nomena et al., 2018). As the oil fraction continues to increase, the droplets appear more homogeneously dispersed across the area imaged. It's noted as well that the CMF network appears less dispersed as oil fraction increases. This is due to the fact that the droplets are incompressible, while the CMF flocs are.

5. Conclusions

This study demonstrates that emulsions can be successfully formed using both cellulose microfibrils (CMF) and potato protein in the continuous phase. Emulsions prepared with 0.5 wt% citrus fibre (which contains CMF) show a droplet size of approximately 5 μm, but significantly smaller droplets are formed when enough potato protein isolate is added. This demonstrates that the CMF is able to stabilise the emulsion droplets, and that as protein concentration increases, the droplet size decreases. The decrease in droplet size leads to an increase in the storage modulus of the emulsion, as the Laplace pressure is increased.

At pH values higher than the isoelectric point (IEP) of the protein ($\geq$5), the storage modulus of the emulsion is significantly lower than at pH values below the IEP ($\leq$4.5). This effect is attributed to aggregation of the potato protein, flocculation of droplets, and electrostatic attraction between the CMF and the protein at the droplet interface. Acidifying the system through the IEP of the protein shifts the droplet's contribution from weakening to strengthening emulsion elasticity.

Increasing the fraction of the dispersed phase within this system (0–40 wt% soybean oil), causes a droplet size increase, due to reduction in the protein concentration per unit surface area of the oil-water interface. The storage modulus of the emulsion at pH 4 increases with increasing oil fraction, but decreases at pH 6, which is indicative of active and inactive filler droplets, respectively.

These emulsions are versatile, as the elasticity of the emulsion can be altered significantly in several different ways, namely protein concentration, pH, and oil fraction. As such, a wide variety of food emulsions can be formulated using these materials as a base. If these materials are to be used for real world applications, further studies on the shelf-life, flavour, and aroma of these samples should be conducted, as these factors were not studied here.

CRediT authorship contribution statement

Ieuan Roberts-Harry: Writing – review & editing, Writing – original draft, Visualization, Methodology, Investigation, Formal analysis, Conceptualization. **Pau Marquès Duran:** Investigation, Formal analysis. **Max Molendijk:** Methodology, Investigation. **Daniel Bonn:** Writing – review & editing, Supervision, Conceptualization. **Krassimir P. Velikov:** Writing – review & editing, Supervision, Methodology, Funding acquisition, Conceptualization.

Declaration of competing interest

The authors declare that they have no known competing financial interests or personal relationships that could have appeared to influence the work reported in this paper.

Acknowledgements

This project has received funding from the European Union's Horizon 2020 research and innovation programme under the Marie Sklodowska-Curie grant agreements No 956248.

Appendix A. Supplementary data

Supplementary data to this article can be found online at https://doi.org/10.1016/j.foodhyd.2025.112348.

Data availability

Data will be made available on request.

References

Bhutto, R. A., Bhutto, N.u. a. H., Khanal, S., Wang, M., Iqbal, S., Fan, Y., & Yi, J. (2024). Potato protein as an emerging high-quality: Source, extraction, purification, properties (functional, nutritional, physicochemical, and processing), applications, and challenges using potato protein. *Food Hydrocolloids, 157*. https://doi.org/10.1016/j.foodhyd.2024.110415

Blok, A. E., Bolhuis, D. P., Kibbelaar, H. V. M., Bonn, D., Velikov, K. P., & Stieger, M. (2021). Comparing rheological, tribological and sensory properties of microfibrillated cellulose dispersions and xanthan gum solutions. *Food Hydrocolloids, 121*. https://doi.org/10.1016/j.foodhyd.2021.107052

Chinga-Carrasco, G. (2011). Cellulose fibres, nanofibrils and microfibrils: The morphological sequence of MFC components from a plant physiology and fibre technology point of view. *Nanoscale Research Letters*. https://doi.org/10.1186/1556-276X-6-417

Costa, A. L. R., Gomes, A., Tibolla, H., Menegalli, F. C., & Cunha, R. L. (2018). Cellulose nanofibers from banana peels as a pickering emulsifier: High-energy emulsification processes. *Carbohydrate Polymers, 194*, 122–131. https://doi.org/10.1016/j.carbpol.2018.04.001

de Gennes, P.-G. (1979). *Scaling concepts in polymer physics*. Cornell University Press.

de Kort, D. W., Veen, S. J., Van As, H., Bonn, D., Velikov, K. P., & van Duynhoven, J. P. (2016). Yielding and flow of cellulose microfibril dispersions in the presence of a charged polymer. *Soft Matter, 12*(21), 4739–4744. https://doi.org/10.1039/c5sm02869h

Derkach, S. R. (2009). Rheology of emulsions. *Advances in Colloid and Interface Science, 151*(1–2), 1–23. https://doi.org/10.1016/j.cis.2009.07.001

Dickinson, E. (2012). Emulsion gels: The structuring of soft solids with protein-stabilized oil droplets. *Food Hydrocolloids, 28*(1), 224–241. https://doi.org/10.1016/j.foodhyd.2011.12.017

Dickinson, E., & Chen, J. (1999). Heat-set whey protein emulsion gels: Role of active and inactive filler particles. *Journal of Dispersion Science and Technology, 20*, 197–213.

Dinkgreve, M., Paredes, J., Denn, M. M., & Bonn, D. (2016). On different ways of measuring "the" yield stress. *Journal of Non-newtonian Fluid Mechanics, 238*, 233–241. https://doi.org/10.1016/j.jnnfm.2016.11.001

Fechner, A., Fenske, K., & Jahreis, G. (2013). Effects of legume kernel fibres and citrus fibre on putative risk factors for colorectal cancer: A randomised, double-blind, crossover human intervention trial. *Nutrition Journal, 12*. https://pubmed.ncbi.nlm.nih.gov/24060277/.

Goudappel, G. J., van Duynhoven, J. P., & Mooren, M. M. (2001). Measurement of oil droplet size distributions in food oil/water emulsions by time domain pulsed field gradient NMR. *Journal of Colloid and Interface Science, 239*(2), 535–542. https://doi.org/10.1006/jcis.2001.7603

Huang, L., Cai, Y., Fang, F., Huang, T., Zhao, M., Zhao, Q., & Van der Meeren, P. (2024). Recent advance in the valorization of soy-based by-products: Extraction, modification, interaction and applications in the food industry. *Food Hydrocolloids, 157*. https://doi.org/10.1016/j.foodhyd.2024.110407

Joyner, H. S. (2018). Explaining food texture through rheology. *Current Opinion in Food Science, 21*, 7–14. https://doi.org/10.1016/j.cofs.2018.04.003

Kam, K. M., Zeng, L., Zhou, Q., Tran, R., & Yang, J. (2013). On assessing spatial uniformity of particle distributions in quality control of manufacturing processes. *Journal of Manufacturing Systems, 32*(1), 154–166. https://doi.org/10.1016/j.jmsy.2012.07.018

Karppinen, A., Saarinen, T., Salmela, J., Laukkanen, A., Nuopponen, M., & Seppälä, J. (2012). Flocculation of microfibrillated cellulose in shear flow. *Cellulose, 19*(6), 1807–1819. https://doi.org/10.1007/s10570-012-9766-5

Krstonošić, V. S., Kalić, M. D., Dapčević-Hadnađev, T. R., Lončarević, I. S., & Hadnađev, M. S. (2020). Physico-chemical characterization of protein stabilized oil-in-water emulsions. *Colloids and Surfaces A: Physicochemical and Engineering Aspects, 602*. https://doi.org/10.1016/j.colsurfa.2020.125045

Liu, C., Pei, R., & Heinonen, M. (2022). Faba bean protein: A promising plant-based emulsifier for improving physical and oxidative stabilities of oil-in-water emulsions. *Food Chemistry, 369*, Article 130879. https://doi.org/10.1016/j.foodchem.2021.130879

Liu, X., Wang, B., Tang, S., Yue, Y., Xi, W., Tan, X., Li, G., Bai, J., & Huang, L. (2024). Modification, biological activity, applications, and future trends of citrus fiber as a functional component: A comprehensive review. *International Journal of Biological Macromolecules, 269*(Pt 1), Article 131798. https://doi.org/10.1016/j.ijbiomac.2024.131798

MacKintosh, F., & Janmey, P. A. (1995). Elasticity of semiflexible biopolymer networks. *American Physical Society*. https://doi.org/10.1103/PhysRevLett.75.4425

Miao, C., Atifi, S., & Hamad, W. Y. (2020). Properties and stabilization mechanism of oil-in-water pickering emulsions stabilized by cellulose filaments. *Carbohydrate Polymers, 248*, Article 116775. https://doi.org/10.1016/j.carbpol.2020.116775

Moon, R. J., Martini, A., Nairn, J., Simonsen, J., & Youngblood, J. (2011). Cellulose nanomaterials review: Structure, properties and nanocomposites. *Chemical Society Reviews, 40*(7), 3941–3994. https://doi.org/10.1039/c0cs00108b

Mudgil, D., & Barak, S. (2013). Composition, properties and health benefits of indigestible carbohydrate polymers as dietary fiber: A review. *International Journal of Biological Macromolecules, 61*, 1–6. https://doi.org/10.1016/j.ijbiomac.2013.06.044

Naz, S., Ahmad, N., Akhtar, J., Ahmad, N. M., Ali, A., & Zia, M. (2016). Management of citrus waste by switching in the production of nanocellulose. *IET Nanobiotechnology, 10*(6), 395–399. https://doi.org/10.1049/iet-nbt.2015.0116

Nomena, E. M., Remijn, C., Rogier, F., van der Vaart, M., Voudouris, P., & Velikov, K. P. (2018). Unravelling the mechanism of stabilization and microstructure of oil-in-water emulsions by native cellulose microfibrils in primary plant cells dispersions. *ACS Applied Bio Materials, 1*(5), 1440–1447. https://doi.org/10.1021/acsabm.8b00385

Nomena, E. M., van der Vaart, M., Voudouris, P., & Velikov, K. P. (2021). Rheology of oil-in-water emulsions stabilised by native cellulose microfibrils in primary plant cells dispersions. *Food Structure, 30*. https://doi.org/10.1016/j.foostr.2021.100239

Olsmats, E., & Rennie, A. R. (2024). Pea protein [pisum sativum] as stabilizer for oil/water emulsions. *Advances in Colloid and Interface Science, 326*, Article 103123. https://doi.org/10.1016/j.cis.2024.103123

Pal, R. (2011). Rheology of simple and multiple emulsions. *Current Opinion in Colloid & Interface Science, 16*(1), 41–60. https://doi.org/10.1016/j.cocis.2010.10.001

Princen, H. M., & Kiss, A. D. (1986). Rheology of foams and highly concentrated emulsions: III. Static shear modulus. *Journal of Colloid and Interface Science, 112*(2), 427–437. https://doi.org/10.1016/0021-9797(86)90111-6

Roberts-Harry, I., Macias-Rodriguez, B. A., & Velikov, K. P. (2026). Use of cellulose microfibrils and potato protein to form double network gels. *Food Hydrocolloids, 172*. https://doi.org/10.1016/j.foodhyd.2025.111958

Tan, Y., Wannasin, D., & McClements, D. J. (2023). Utilization of potato protein fractions to form oil-in-water nanoemulsions: Impact of pH, salt, and heat on their stability. *Food Hydrocolloids, 137*. https://doi.org/10.1016/j.foodhyd.2022.108356

van Koningsveld, G. A., Walstra, P., Voragen, A. G., Kuijpers, I. J., van Boekel, M. A., & Gruppen, H. (2006). Effects of protein composition and enzymatic activity on formation and properties of potato protein stabilized emulsions. *Journal of Agricultural and Food Chemistry, 54*(17), 6419–6427. https://doi.org/10.1021/jf061278z

Waglay, A., & Karboune, S. (2016). Potato proteins. In *Advances in potato chemistry and technology* (pp. 75–104). https://doi.org/10.1016/b978-0-12-800002-1.00004-2

Wallecan, J., McCrae, C., Debon, S. J. J., Dong, J., & Mazoyer, J. (2015). Emulsifying and stabilizing properties of functionalized orange pulp fibers. *Food Hydrocolloids, 47*, 115–123. https://doi.org/10.1016/j.foodhyd.2015.01.009

Wang, C., Cao, X., Liu, J., Yan, S., Zhou, G., Ding, C., & Zhuang, X. (2025). Insight into the mechanism of heat-induced gelation improved by soybean protein isolate/bacterial cellulose co-assemblies: Spatial distribution and three-dimensional networks. *Food Hydrocolloids, 162*. https://doi.org/10.1016/j.foodhyd.2024.110993

Yuan, T., Zeng, J., Wang, B., Cheng, Z., & Chen, K. (2021). Pickering emulsion stabilized by cellulosic fibers: Morphological properties-interfacial stabilization-rheological behavior relationships. *Carbohydrate Polymers, 269*, Article 118339. https://doi.org/10.1016/j.carbpol.2021.118339

Zhang, S., Du, R., Li, Q., Xu, M., Yang, Y., Fang, S., Wan, Z., & Yang, X. (2024). Food-grade emulsion gels and oleogels prepared by all-natural dual nanofibril system from citrus fiber and glycyrrhizic acid. *Food Research International, 192*, Article 114830. https://doi.org/10.1016/j.foodres.2024.114830

Zhang, X., Wu, Y., Li, Y., Li, B., Pei, Y., & Liu, S. (2022). Effects of the interaction between bacterial cellulose and soy protein isolate on the oil-water interface on the digestion of the pickering emulsions. *Food Hydrocolloids, 126*. https://doi.org/10.1016/j.foodhyd.2021.107480

Zhang, T., Xu, J., Chen, J., Wang, Z., Wang, X., & Zhong, J. (2021). Protein nanoparticles for pickering emulsions: A comprehensive review on their shapes, preparation methods, and modification methods. *Trends in Food Science & Technology, 113*, 26–41. https://doi.org/10.1016/j.tifs.2021.04.054

Zhu, M., Wang, H., Sun, T., Lv, J., Wang, K., Huan, S., Li, Z., Liu, Y., Liu, S., McClements, D. J., & Bai, L. (2025). Plant-based pickering emulsions using cellulose nanofibers and soy protein isolate: Stabilization and high environmental resistance. *Food Hydrocolloids, 162*. https://doi.org/10.1016/j.foodhyd.2024.110943